

# Supporting Information

## Stable *peri*-Xanthenoxanthene Thin-Film Transistors with Efficient Carrier Injection

Norihito Kobayashi,\* Mari Sasaki and Kazumasa Nomoto

Organic Electronics Research Laboratory, Advanced Materials Laboratories, Sony Corporation,  
Atsugi, 243-0021, Japan

E-mail: Norihito.Kobayashi@jp.sony.com

### Optical microscope image

In Figure S1, the optical microscope image of the PXX-deposited sample is shown. PXX was vacuum-deposited on the substrate. However, many single crystals were grown on the surface of the substrate.

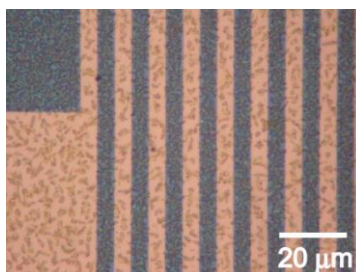


**Figure S1.** Optical microscope image of the PXX deposited on a substrate with Au electrodes.

### <sup>1</sup>H-NMR

<sup>1</sup>H NMR spectra of Br-PXX, Ph-PXX and PrPh-PXX are shown in Figure S2, S3 and S4, respectively. THF-*d*8 was used as the solvent.

In Figure S3(b), the time dependence of <sup>1</sup>H-NMR spectrum are shown. The spectra were not changed for 5 days. The NMR sample was stored at the ambient conditions, following the NMR measurement as the initial data.

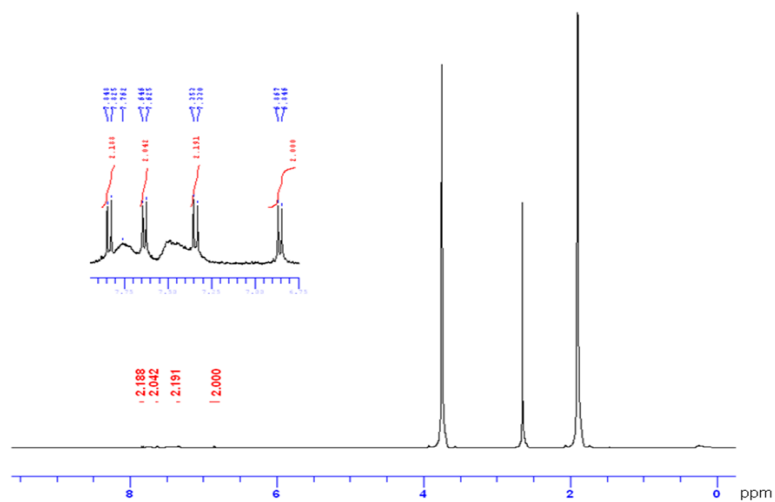
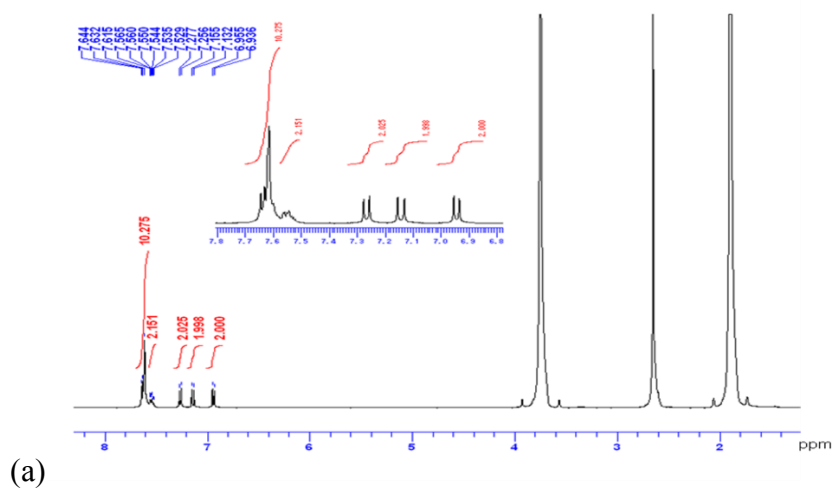
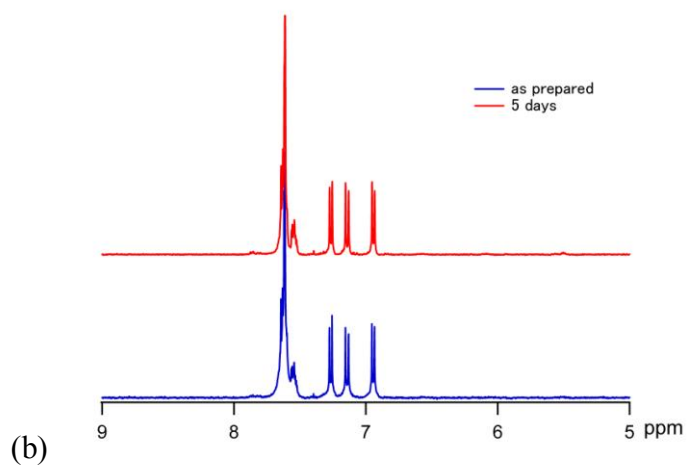


**Figure S2.**  $^1\text{H-NMR}$  spectrum of Br-PXX in  $\text{C}_4\text{D}_8\text{O}$ .



(a)



(b)

**Figure S3.** a)  $^1\text{H-NMR}$  spectrum of Ph-PXX in  $\text{C}_4\text{D}_8\text{O}$ . b) Time dependence of  $^1\text{H-NMR}$  spectrum.

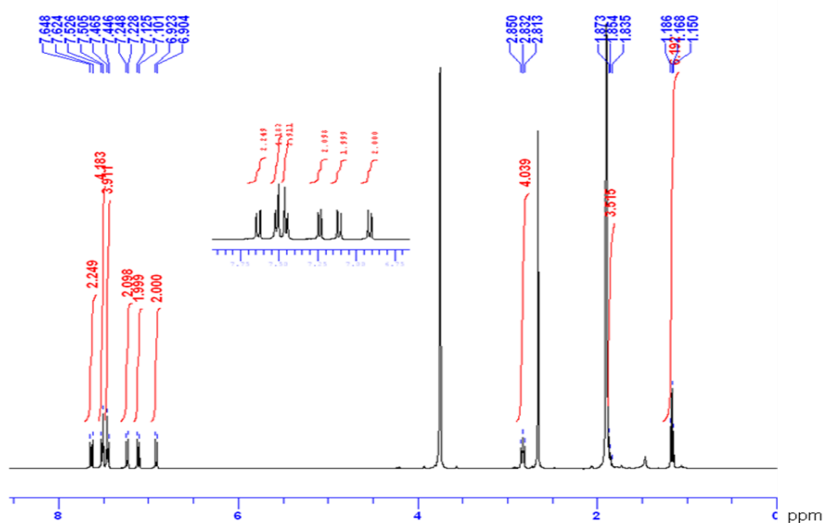


Figure S4.  $^1\text{H}$ -NMR spectrum of PrPh-PXX in  $\text{C}_4\text{D}_8\text{O}$ .

### Molecular orbital calculation

MO calculations were carried out by density functional theory (DFT) methods at the B3LYP-6-31G(d,p) level using a Gaussian, *Inc.* Gaussian R 03W ver. 6.0.

Calculated IP of anthanthrene, PXX and Ph-PXX were 6.3S1, 6.19 and 5.96 eV, respectively. The distribution of the HOMO of each molecule was shown in Figure S2.

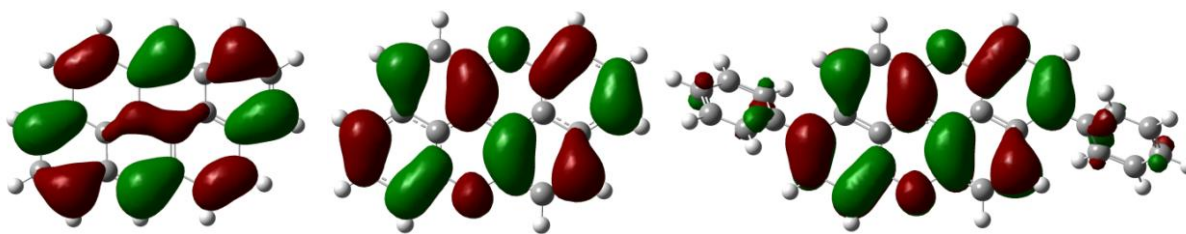
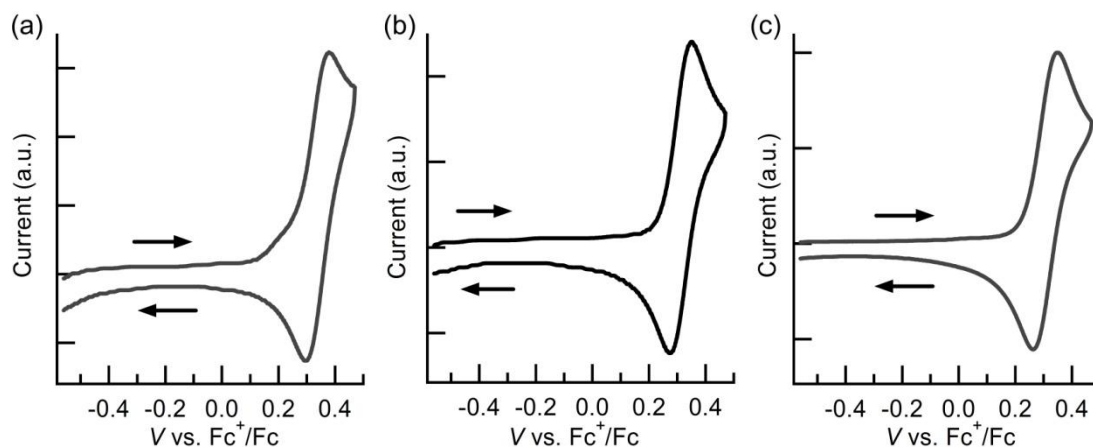


Figure S5. Distribution of the HOMO of anthanthrene, PXX and Ph-PXX (from left).

### Cyclic Voltammetry

Measurements were recorded with tetrabutylammonium hexafluorophosphate ( $\text{TBAPF}_6$ , 0.1 M) as supporting electrolyte. The scan rate was 100 mV/s. Counter and working electrodes consisted of Pt and carbon, respectively. The reference electrode was Ag/AgCl, and the potential was calibrated using the  $\text{Fc}/\text{Fc}^+$  redox couple ( $E^{1/2} = +0.48$  V measured under identical conditions).



**Figure S6.** CVs of (a) PXX, (b) Ph-PXX and (c) PrPh-PXX in benzonitrile.

## TGA and DSC

Thermogravimetric analysis (TGA) was performed using a TA Instruments Q500. Differential scanning calorimetry (DSC) was carried out on a Seiko Instruments, *Inc.* DSC 6200. The TGA and DSC traces of Ph-PXX are shown in Figure S4.

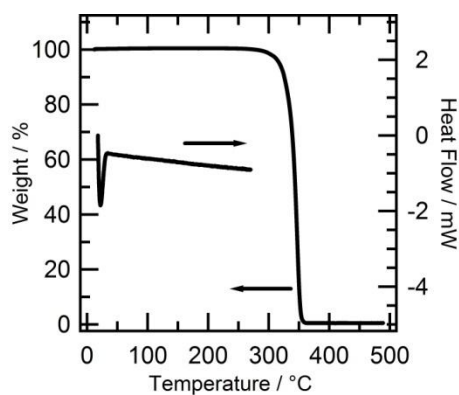


**Figure S7.** TGA and DSC traces of Ph-PXX.

## Single Crystal X-ray Analysis

The single crystal of Ph-PXX was obtained by vacuum sublimation. The X-ray single crystal structure analysis was carried out on a Bruker AXS SMART APEX II diffractometer system (graphite monochromated MoK $\alpha$  radiation,  $\lambda = 0.71069$  Å,  $T = 298$  K).

Crystal data for Ph-PXX: C<sub>32</sub>H<sub>18</sub>O<sub>2</sub>,  $M_w = 434.46$ , yellow, needle,  $0.20 \times 0.10 \times 0.05$  mm<sup>3</sup>, orthorhombic, space group *Pccn*,  $a = 15.920(2)$ ,  $b = 18.508(3)$ ,  $c = 6.9299(9)$  Å,  $V = 2041.9(5)$  Å<sup>3</sup>,  $Z = 4$ ,  $D_{\text{calc}} = 1.413$  gcm<sup>-3</sup>,  $R = 0.0505$  for 2338 observed reflections ( $I > 2\sigma(I)$ ) and 150 variable parameters,  $R_w = 0.1431$  for

all data. Non-hydrogen atoms were refined anisotropically, and hydrogen atoms were included in the calculations.

Molecular structure is shown in Figure S8. Crystal structures are shown in Figure S9.

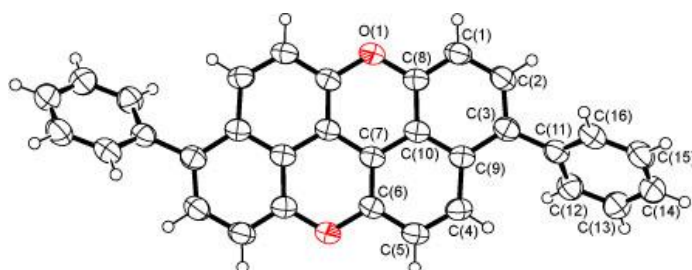


**Figure S8.** Molecular structure of Ph-PXX.

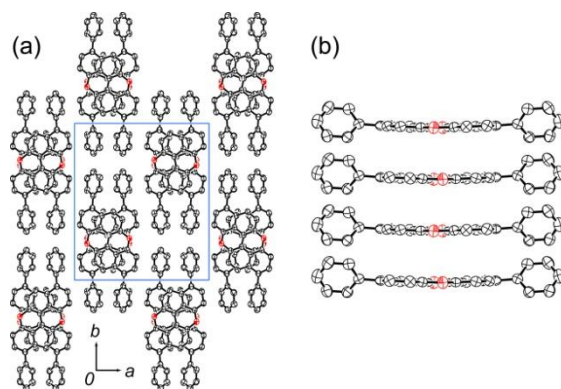


**Figure S9.** (a) Crystal structure of Ph-PXX. (b) View perpendicular to face-to-face stacking column of Ph-PXX.

## XRD

Out-of-plane X-ray diffractions (XRDs) were obtained with a RIGAKU ATX-G diffractometer with a Cu  $K\alpha$  source ( $\lambda = 1.541 \text{ \AA}$ ) in the air.  $\omega/2\theta$  scans were performed. XRD pattern of evaporated Ph-PXX film on PVP is shown in Figure S10.

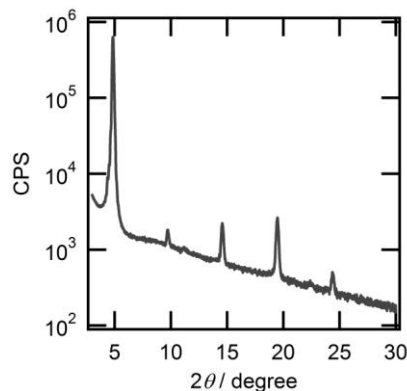


**Figure S10.** XRD pattern of evaporated Ph-PXX film. The  $d$ -space was calculated as  $18.2 \text{ \AA}$  ( $2\theta = 4.86^\circ$ ).

## FET Device Evaluations

Pentacene was vacuum-deposited on a PVP gate dielectric. Transfer characteristics and the effect of annealing are shown in Figure S11. Ph-PXX was vacuum-deposited on Si substrate with a PVP gate dielectric. The annealed device was stored under ambient conditions for five months. The transfer characteristics are shown in Figure S12. PrPh-PXX was vacuum-deposited on a PVP gate dielectric. TFT characteristics are shown in Figure S13.

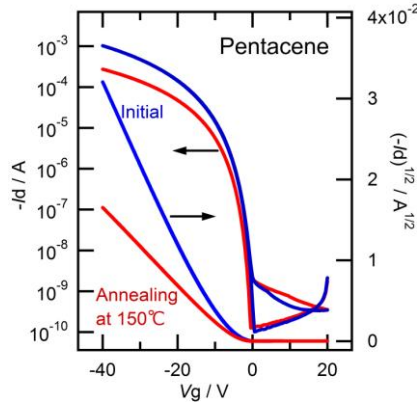


**Figure. S11.** Transfer characteristics of pentacene TFT fabricated on a PVP gate insulator.

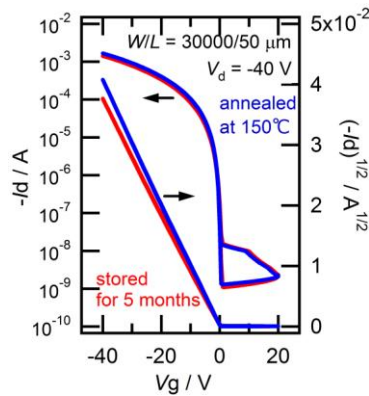


**Figure S12.** (a) Transfer characteristics of the Ph-PXX TFT (blue) after annealing and (red) after storing for 5 months.

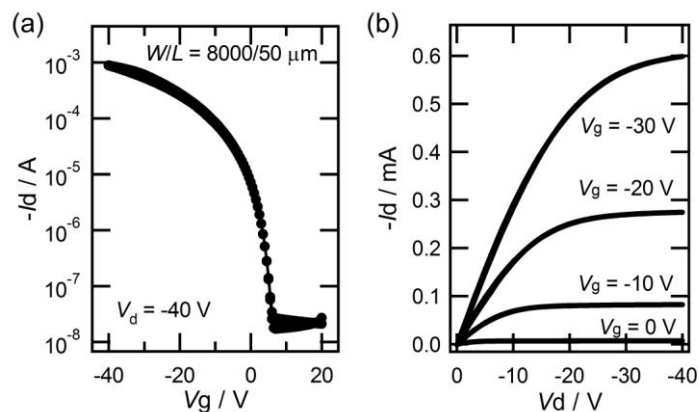


**Figure S13.** (a) Transfer and (b) output characteristics of the TFT with vacuum-deposited PrPh-PXX on a PVP gate insulator.